J. Fluid Mech. (1967), *vol.* 29, *part* 3, *pp.* 495–512
Printed in Great Britain

Experiments on a turbulent cylindrical wall jet

By J. B. STARR† AND E. M. SPARROW
University of Minnesota, Minneapolis, Minnesota

(Received 14 June 1966 and in revised form 3 November 1966)

The investigation described here is an experimental study directed toward determining flow field and surface friction characteristics of a cylindrical wall jet. The flow configuration is obtained by placing a cylindrical rod along the axis of a converging nozzle. The flow field thus produced consists of a developing turbulent boundary layer co-existing with an outer fluid layer that mixes freely with quiescent surroundings. Direct measurements of fluid friction at the rod surface, performed with a hot-film element, revealed a significant effect of transverse surface curvature on the local friction factor. Velocity profiles at various axial stations exhibited similarity in the outer mixing layer, but not in the boundary layer adjacent to the surface. Representations of the velocity field in terms of law of the wall variables and defect-law variables revealed significant transverse curvature effects. The measured wall-jet velocity profiles could be satisfactorily represented in terms of a law of the wake, wherein the wake function depends on a transverse curvature parameter. In the outer mixing layer, the eddy viscosity data correspond closely to those of free jets.

1. Introduction

Numerous fluid flow and heat transfer processes involve the interaction of a fluid jet with a solid surface. In many cases, there results from this interaction a fluid layer which is bounded, in part, by the solid surface, but which also mixes freely with otherwise quiescent fluid surroundings. Such a flow configuration is commonly called a 'wall jet'. For example, a wall jet is formed by the fluid layer which spreads out radially from an axisymmetric jet impinging normal to a solid surface.

There are, of course, a wide range of jet-surface configurations wherein wall-jet flows are produced. The published literature deals primarily with two configurations, the plane wall jet and the radial wall jet. Lesser consideration has been accorded to the cylindrical wall jet. As indicated in figure 1, a cylindrical wall jet is created when a jet emerges from an annular slot and flows longitudinally and co-axially about a cylindrical rod situated in an otherwise quiescent environment.

Experimental investigations of wall jets have dealt exclusively with the case of turbulent flow, the laminar case being infrequently encountered owing to the low critical Reynolds number for free mixing layers. The earliest experimental exploration of plane wall-jet flows appears to have been carried out by Förthmann

† Present address: Fluid Sciences Section, S and R Division, Honeywell Inc.

(1934). In more recent years, experimental studies of this flow configuration were performed by Sigalla (1958), Bradshaw & Gee (1960), Schwarz & Cosart (1961), Mathieu & Tailland (1961, 1963), Myers, Schauer & Eustis (1963) and Kruka & Eskinazi (1964). For the radial wall jets, experiments are reported by Bakke (1957) and by Bradshaw & Love (1961). While there is some discrepancy among the results of the various investigations, sufficient agreement does exist so as to provide reasonable estimates of surface friction coefficients, streamwise development characteristics, and velocity profile shapes.

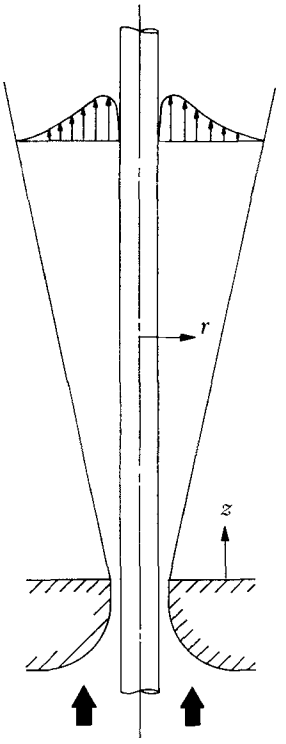

FIGURE 1. Cylindrical wall jet configuration.

In contrast to the aforementioned availability of information for both plane and radial wall jets, the only experiment reported in the literature for a cylindrical wall jet is that of Lawrence (1964). However, only sparse data are presented and these are in the form of dimensionless velocity profiles, thereby yielding no information concerning streamwise development and surface friction characteristics. An adequate description of cylindrical wall-jet flows is important to the general body of knowledge of wall jets since it represents a configuration possessing transverse surface curvature. However, aside from the profiles reported by Lawrence, there is currently no experimental data available to even qualitatively suggest what the effects of transverse curvature might be.

Analyses of the turbulent wall jet have been carried out by Glauert (1956) for the plane and radial cases and by Myers *et al.* (1963) for the plane case only. In both analyses, it is assumed that the region between the wall and the point of

maximum velocity is similar to a turbulent flat-plate boundary layer, while the region beyond that point possesses the characteristics of a free mixing layer. Inherent in these assumptions is a discontinuity in the structure of the turbulence at the point of maximum velocity. In addition, both analyses utilize the Blasius expression for turbulent shear at the surface; this model results in surface friction coefficients that are approximately 25 % below experimental wall-jet values. Spalding (1965) has proposed an extension of Coles's law of the wake to include wall-jet flows. The results of this approach have provided good estimates of surface friction coefficients for plane wall jets. Further, by employing Head's (1958) entrainment theory, a reasonable description of the streamwise development of the plane wall jet is obtained. However, the velocity profile shapes which result are not in good agreement with experimental data.

The foregoing review of wall-jet analyses therefore shows that the models employed do not yield fully satisfactory predictions. Consequently, applications of these analyses cannot be made with confidence where experimental data is lacking.

On the basis of the remarks of the previous paragraphs, it is evident that data from a thoroughgoing experimental investigation of a cylindrical wall jet are needed to provide insight into the problem of wall-jet flows over surfaces possessing transverse curvature. For this reason, the present investigation was undertaken. Measurements were performed which provide detailed information on both the transverse and streamwise characteristics of the velocity field and on the fluid shear at the surface of the cylindrical rod. The experimental data are employed in evaluating the momentum exchange characteristics of the flowing fluid. The measured velocity field is represented in terms of the law of the wall, the defect law, and the law of the wake, and the adequacy of the various representations assessed. Wherever possible, flow phenomena related to the transverse curvature of the surface are delineated.

2. Apparatus, instrumentation, and measurement technique

The experimental apparatus

The apparatus employed to create a cylindrical wall jet consisted of a $\frac{1}{2}$ in. diameter polished stainless steel rod issuing concentrically from a carefully machined converging nozzle designed to be free of flow separation. The exit diameter of the nozzle was 0·667 in., thereby leaving an annular gap of 0·083 in. The rod had a total length of 12 ft. and was oriented vertically in order to eliminate the possibility of sag. Flow field measurements were made along a 32 in. section downstream of the nozzle; the remaining portion of the rod served for support and alignment. The mounting system for the rod was so designed as to permit its vertical movement (as will be discussed later, this feature was employed in the measurement of the fluid shear at the rod surface). In addition, a fine adjustment in the transverse positioning of the rod was provided to facilitate its alignment.

A plenum chamber containing a series of screens and baffles provided a uniform flow field upstream of the nozzle. The uniformity of the flow was verified by measurement.

The air flow supplied to the apparatus from a general supply system, was precisely regulated so as to give a steady nozzle exit velocity. A temperature control system consisting of an ice bath and a low-wattage heater was employed to maintain the air temperature to within $\frac{1}{4}$ °F of that of the room. Mass flow rates were measured by means of a calibrated orifice installed upstream of the plenum.

Vertical alignment of the rod was accomplished optically with the aid of a surveyor's transit, while a specially designed mechanical gauge facilitated concentric alignment of the rod with the nozzle to within 0·0005 in. In addition, axial symmetry of the flow field was checked by a pair of impact probes which, when mounted on the rod, could be rotated through circles concentric with the rod.

Various details of the test apparatus have been omitted here in the interest of a concise presentation. Further information is available in Starr (1966).

Instrumentation

Velocities in the flow field of the wall jet were measured with an impact probe fabricated from stainless steel hypodermic tubing. The probe tip was drawn and flattened so as to form a rectangular opening of 0·003 by 0·032 in., with an overall tip height of 0·008 in. The probe was mounted on a traversing mechanism which provided for both horizontal and vertical movements at any circumferential station. Carefully controlled horizontal positioning in perpendicular directions was accomplished using two lead screws equipped with dials calibrated to 0·001 in. A third lead screw facilitated vertical positioning to within 0·01 in. Contact of the probe with the rod surface was detected by electrical continuity.

Static and impact pressures were displayed by oil-filled manometers. Pressure levels of up to 4 in. of oil were read to within 0·001 in. using a Gaertner travelling microscope, while levels in excess of 4 in. of oil were read to within 0·01 cm with a Gaertner cathetometer.

The direct measurement of the fluid shear stress was accomplished using a hot-film element which consists, in general, of a small heater (e.g. a wire or strip) embedded in a surface at the point where the fluid shear stress is to be measured. The technique, originated by Ludwieg (1950), is based on the hypothesis that there exists a region near the wall (i.e. the so-called laminar sublayer) where the flow-field characteristics are uniquely determined by the wall shear stress. If this region completely contains the thermal boundary layer developing adjacent to the heated element, then the heat transfer coefficient for the element is a function of the wall shear stress.

The hot-film element designed and employed in this investigation consists essentially of an 0·003 in. diameter platinum wire embedded at the surface of a layer of epoxy which fills a circumferential groove in the $\frac{1}{2}$ in. diameter rod. With the rod-mounting system as previously mentioned, the hot-film element could be positioned at any level above the nozzle up to 34 in. by moving the entire rod assembly.

An electrical circuit was designed, wherein the platinum wire formed one branch of a Wheatstone bridge. Precision laboratory instruments could then be employed to determine accurately both the current through the wire and the wire

resistance. In an auxiliary experiment performed with the wire in place, the resistance–temperature relationship was established.

Calibration of the hot-film element was carried out using a concentric annular duct formed by shrouding the $\frac{1}{2}$ in. diameter rod with a 0·915 in. I.D. seamless brass tube whose length was 30 in. It was established by static pressure measurements† that fully developed turbulent flow existed in the downstream half of the duct; consequently, in this region the overall wall shear force was proportional to the static pressure gradient. In addition, the location of the maximum velocity in the cross-section was ascertained from velocity profile measurements† near the duct exit, thus furnishing the necessary additional information required in the computation of the shear stress at the rod surface.

The aforementioned calibration provided the relationship between the fluid shear at the rod surface and the heat transfer coefficient for the heated element. An exhaustive analytical investigation‡ was carried out in order to determine if a calibration performed in an annular duct flow would apply to the cylindrical wall jet. In particular, the following factors were considered: (1) changes in turbulent structure, (2) variations in transverse shear stress distribution, (3) the existence of a transverse velocity component, and (4) changes in the contribution of longitudinal heat conduction in the fluid. These factors were found to have no more than a second-order effect on the calibration, thereby lending support to the accuracy of the data.

Velocity-field measurement technique

Flows with mixing layers are inherently unsteady. In the present investigation, this unsteadiness was manifested as a timewise fluctuation of the pressure signal from the impact probe, particularly in the outer mixing layer. In view of this, a sampling procedure was evolved on the basis of a statistical analysis of the observed pressure fluctuations. It was found that by successively recording data spaced at given intervals in time (greater than the time constant of the pressure detection system), the fluctuations appeared random. A sufficient number of these random readings were averaged so as to approximate closely the value corresponding to the average of a sample of infinite size.

In spite of painstaking efforts, perfect symmetry of the flow field could not be achieved. Consequently, velocity data at a given axial station were collected along four equally spaced radial lines (i.e. 90 degrees apart). The four data points corresponding to any given radial distance from the rod surface were averaged; in this way, velocity profiles were determined.

3. Presentation and discussion of results

The velocity field

The first aspect of the velocity field to be considered is profile similarity (congruence of shape of profiles at different axial stations). For plane and radial wall jets,

† In general, the annular flow data from this investigation were in good agreement with experimental results reported by Jonsson (1965) and by Brighton & Jones (1964).

‡ The reader is referred to Starr (1966) for details of the analysis.

substantial experimental evidence of similarity is found in the literature. To examine the similarity of the velocity field of a turbulent cylindrical wall jet, dimensionless velocity profiles have been constructed as shown in figure 2. This figure is representative of more extensive information presented by Starr (1966) consisting of ten profiles at each of two nozzle exit velocities.

For each profile, corresponding to a given axial station, velocities have been normalized by w_m, the maximum velocity† at that station. Furthermore, the transverse co-ordinate y is made dimensionless by $\delta_{\frac{1}{2}}$, which corresponds to the y-value† where $w = \frac{1}{2}w_m$. The data appearing in the figure are for a $Re_N = W\sqrt{A_N}/\nu = 50{,}000$ where W is a momentum-averaged nozzle exit velocity‡ and A_N is the nozzle exit area.

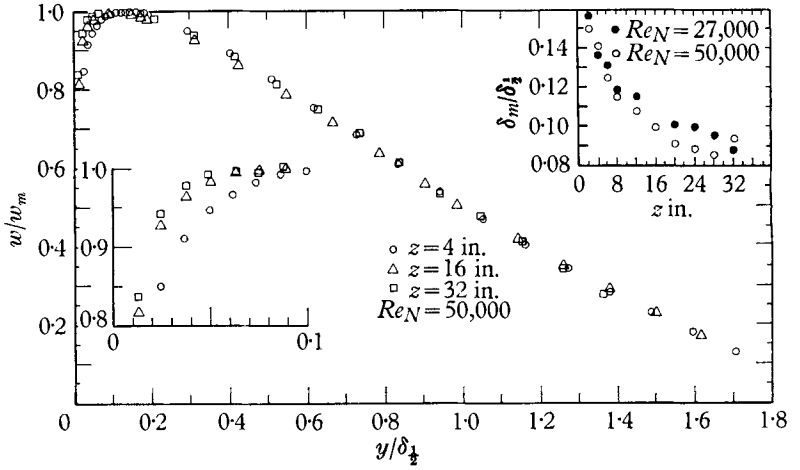

FIGURE 2. Dimensionless velocity profiles.

From an inspection of the figure, it is seen that in the outer mixing layer ($y > \delta_m$) there is similarity of the various profiles. However, in the inner layer, the profiles are definitely non-similar. The non-similar behaviour, which is a manifestation of transverse curvature, is shown more clearly in the inset at the left of the figure.

Further evidence of the non-existence of similarity is obtained from an examination of the thickness parameters $\delta_{\frac{1}{2}}$ and δ_m. At the right of figure 2, a plot of $\delta_m/\delta_{\frac{1}{2}}$ as a function of z departs significantly from a horizontal line that would indicate similarity.

The streamwise development of the flow field is revealed by consideration of jet spread and velocity decay as shown in figure 3. The abscissa variable z_* is the downstream distance measured from the virtual origin of the jet. This virtual origin was found to be 1 in. upstream of the nozzle exit by extrapolating curves of $\delta_{\frac{1}{2}}$ and δ_m versus z to zero thickness. The data indicate that $\delta_{\frac{1}{2}}$ varies as $z_*^{1\cdot07}$ at

† w_m and δ_m (y-value at which $w = w_m$) were evaluated at the point of zero slope of a second-degree polynomial in $\log y$ fitted to 13 velocity data points in the vicinity of $y = \delta_m$. $\delta_{\frac{1}{2}}$ was determined from a Gaussian error curve fitted to 6 data points in the vicinity of $w = \frac{1}{2}w_m$.

‡ In general, W is within $1\frac{1}{2}\%$ of the mass-averaged nozzle exit velocity.

both nozzle Reynolds numbers. Thus, the spread characteristics of a cylindrical wall jet correspond closely to those of free jets and plane wall jets, which are also described by an exponent near 1·0.

Experimental data have shown that the streamwise variation of the peak velocity in plane wall jet velocity profiles can be expressed by

$$w_m \sim z_*^{-n}, \tag{1}$$

where n is near 0·5. However, the w_m/W data from the present investigation, presented in figure 3, do not fall on a straight line at either Reynolds number. Consequently, correlation by a simple expression involving only z_* to a fixed power is not possible. In seeking an analytical model to describe the measured results for the cylindrical wall jet, we note that both plane free jets and plane wall jets are characterized by an n-value near 0·5. Thus, it appears that the effect

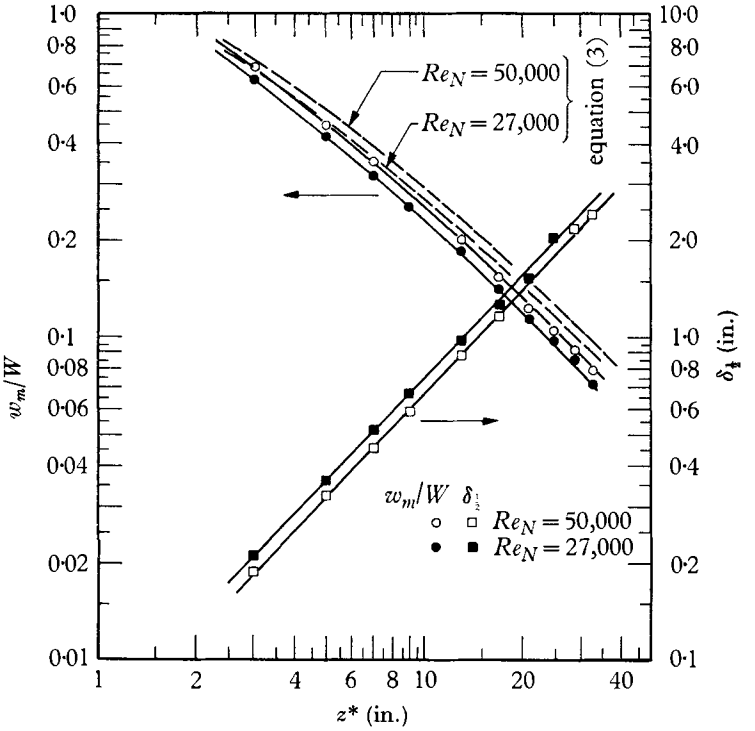

FIGURE 3. Streamwise development of wall-jet flow field.

of the bounding surface of the streamwise development of a wall jet is small. On the basis of this finding, a quantitative characterization of the velocity decay characteristics of a cylindrical wall jet can be obtained by employing an analytical model wherein wall effects are ignored.

The model is formulated by assuming that the outer mixing layer extends to the wall, and that $\tau_w = 0$. One begins by writing a momentum balance for an element transversely spanning the flow field and having an axial length dz_*. A reasonable representation of the velocity profile is

$$w/w_m = \exp\{-0{\cdot}692(y/\delta_{\frac{1}{2}})^2\}. \tag{2}$$

The incorporation of this profile into the integral momentum equation plus the assumption that $\delta_{\frac{1}{2}} = \sigma z_*$ (σ = const.) leads to the expression

$$w_m = \frac{C}{[0{\cdot}361\,(\delta_{\frac{1}{2}}/r_w)^2 + 0{\cdot}753\,(\delta_{\frac{1}{2}}/r_w)]^{\frac{1}{2}}}, \tag{3}$$

where r_w is the radius of the cylindrical rod. The constant C is evaluated by requiring that the total momentum in the flow field at every axial station be equal to the momentum at the nozzle exit. This results in the relation

$$C = W\{\tfrac{1}{2}[(r_N/r_w)^2 - 1]\}^{\frac{1}{2}} \tag{4}$$

where r_N is the nozzle exit radius.

Upon recalling that $\delta_{\frac{1}{2}} = \sigma z_*$, it is deduced from (3) that for $\delta_{\frac{1}{2}}/r_w$ near zero (i.e., a plane wall jet), $w_m \sim z_*^{-\frac{1}{2}}$; whereas for $\delta_{\frac{1}{2}}/r_w$ approaching infinity, $w_m \sim z_*^{-1}$. This change in the relationship between w_m and z_* with increasing downstream distance is an evident manifestation of the effect of transverse curvature.

By use of the experimental data for $\delta_{\frac{1}{2}}$, the dashed lines in figure 3 were generated from (3) and (4). The qualitative agreement of the analytical curves with the experimental data is evident, although the deviations become larger with increasing z. This discrepancy is attributed to neglecting the effect of wall shear stress in the analysis, the shear effects accumulating as z increases.

The data in figure 3 indicate a moderate influence of nozzle Reynolds number on streamwise development. It is believed that this difference in streamwise development stems from a change in the rate of fluid entrainment as related to the total flow rate at the jet source.

Wall shear stress

It is customary to represent wall shear stress data for wall jets in terms of a local friction coefficient c_{fm} defined as

$$c_{fm} = \tau_w/\tfrac{1}{2}\rho w_m^2. \tag{5}$$

Shear stress data from plane wall jet experiments have been correlated by an expression of the form

$$c_{fm} = K(Re_m)^{-n}, \tag{6a}$$

where $Re_m = w_m\,\delta_m/\nu$. Sigalla (1958) found that n and K should be 0·25 and 0·0565 respectively, independent of z. When results of the present investigation were expressed in terms of c_{fm}, no combination of n and K could be found that would adequately describe the data at all z.

In an analysis of turbulent boundary-layer development longitudinal to a circular cylinder, Sparrow, Eckert & Minkowycz (1963) deduced that the effect of transverse curvature on the surface friction coefficient is uniquely related to the parameter $r_w^+ = r_w(\tau_w/\rho)^{\frac{1}{2}}/\nu$. Anticipating that the c_{fm} data from the present investigation are affected by transverse surface curvature, (6a) was rewritten as

$$c_{fm} = (K + K^*)(Re_m)^{-n}, \tag{6b}$$

where K^* was assumed to be a function r_w^+ alone. With $K = 0{\cdot}0565$ and $n = 0{\cdot}25$, K^* values were computed to bring coincidence between the data from the present investigation and (6*b*). The graphical presentation in figure 4 indicates that K^* is related to r_w^+ by the expression

$$K^* = 48{\cdot}1(r_w^+)^{-1{\cdot}27}. \tag{7}$$

Although (7) is empirical, examination of the data in figure 4 gives a strong indication of generality. For example, at an r_w^+ of approximately 290 are two data points taken at different nozzle Reynolds numbers. The data point for $Re_N = 27{,}000$ was recorded at $z = 12$ in. where $\delta_{\frac{1}{2}} = 0{\cdot}98$ in.; the data point for $Re_N = 50{,}000$ was recorded at $z = 24$ in. where $\delta_{\frac{1}{2}} = 1{\cdot}83$ in. In other words, the correlation expressed by (7) does not appear to be sensitive to the details of the local flow field.

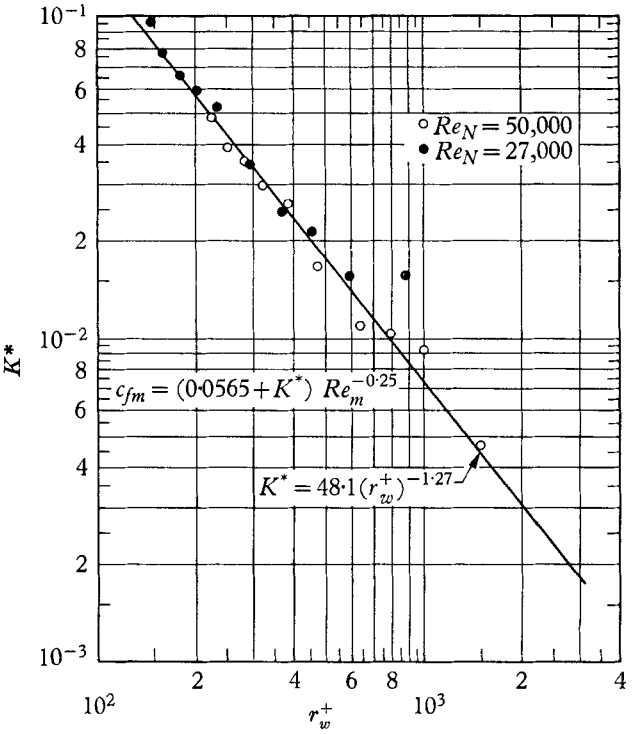

FIGURE 4. Correlation of K^* with r_w^+.

Law of the wall and defect-law representations

In many turbulent boundary-layer investigations, velocity data are represented in terms of wall-law variables in the form

$$w^+ = f(y^+), \tag{8}$$

where

$$w^+ = w/(\tau_w/\rho)^{\frac{1}{2}}, \quad y^+ = y(\tau_w/\rho)^{\frac{1}{2}}/\nu. \tag{8a}$$

Wall-law plots of velocity data from the present investigation are shown in figure 5, the graphs on the left and on the right being respectively for nozzle Reynolds numbers of 27,000 and 50,000. Also shown for purposes of reference is Coles's (1956) law of the wall. Investigators of the plane wall jet ($r_w^+ = \infty$) have generally reported data which lie either close to or somewhat above the aforementioned lines. In this light, departures of the present data below the reference lines can be taken as an indication of the transverse curvature effect.

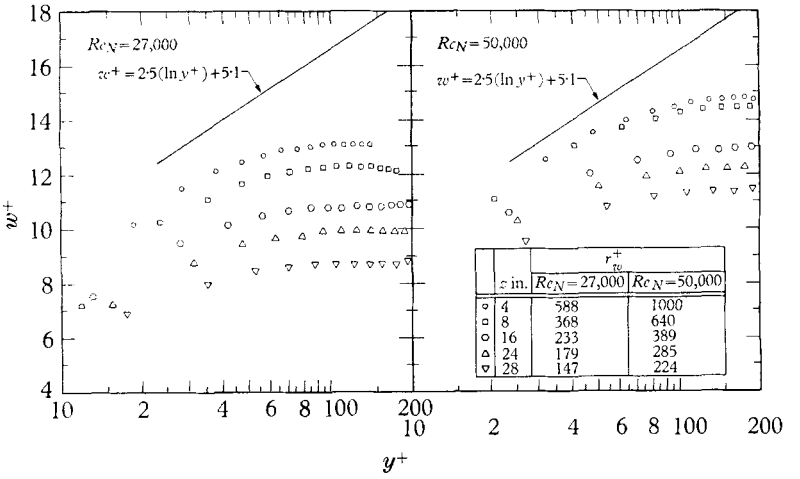

FIGURE 5. Wall-law representation of velocity data.

Departures from Coles's wall-law expression are much in evidence even at small y^+ values (e.g. $y^+ = 30$), thereby indicating a first-order effect of transverse curvature. The extent of the deviations are greater at smaller values of the transverse curvature parameter r_w^+. The dependence of the results on r_w^+ is consistent with the prior finding that c_{fm} depends on r_w^+ (note that $w_m^+ = (2/c_{fm})^{\frac{1}{2}}$).

Townsend (1956) has suggested that the existence of an apparent universal wall-law correlation is a consequence of an equilibrium between turbulent energy generation and dissipation *within* the boundary layer. A correlation of this type is not applicable when there is considerable diffusion of turbulent energy into the boundary layer from the external flow field, such as may well occur in the wall jet. Since, in figure 5, separation of the data is related to r_w^+, it is possible that the relative magnitude of diffusion of turbulent energy into the region near the wall is also related to r_w^+.

Correlations of the velocity data by a defect-law representation were attempted with y respectively normalized by $\delta_{\frac{1}{2}}$, δ_0 (y-value where $\tau/\tau_w = 0$) and δ_m.† Among these, the best correlation was obtained using δ_m. Even so, the results presented in figure 6 are less than satisfactory.

The solid curves shown in figure 6 represent a fairing of boundary layer and channel flow data compiled by Klebanoff & Diehl (1952). That the channel flow curve lies below the boundary-layer curve is attributed to the interaction of the

† Some investigators have found that δ_0 and δ_m do not correspond. A subsequent discussion covers this point.

turbulent fluid layers on either side of the channel centreline. On the basis of this explanation, the even lower position of the wall-jet data from the present investigation is attributable to the existence of a flow field of relatively high turbulence intensity in the region $y > \delta_m$ (i.e. the outer mixing layer).

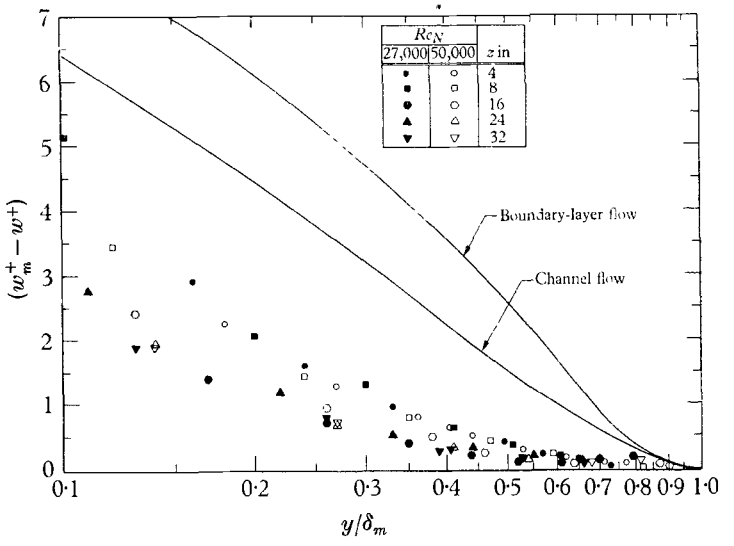

FIGURE 6. Deflect-law representation of velocity data.

Law of the wake representation

On the basis of an extensive examination of available turbulent boundary-layer data, Coles (1956) proposed a universal s-shaped wake function $\omega(y/\delta)$ such that velocity profiles could, in general, be represented by

$$w^+ = [2{\cdot}5\,(\ln y^+) + 5{\cdot}1] + C\omega(y^+/\delta^+), \tag{9}$$

where $\omega(1) = 1$† and $\omega(0) = 0$. This expression is essentially a law of the wall equation modified by the wake function.

Spalding (1965) extended Coles's hypothesis to include turbulent wall jets. For that flow situation, the procedure followed by Spalding is equivalent to evaluating the constant in (9) by setting $w^+ = 0$ at $y^+ = \delta^+$. Following this procedure, there results

$$w^+ = 2{\cdot}5\,(\ln y^+) + 5{\cdot}1 - [2{\cdot}5\,(\ln \delta^+) + 5{\cdot}1]\omega(y^+/\delta^+). \tag{10}$$

Spalding proposed that ω should be of the form

$$\omega = \tfrac{1}{2}(1 - \cos \pi y^+/\delta^+)\,. \tag{11}$$

However, when this function was applied to the plane wall-jet case, significant differences were found to exist between the resulting profile and the experimental data of Bradshaw & Gee (1960). Spalding suggested that a more discreet selection of a wake function would alleviate this discrepancy.

Rather than test various provisional wake functions for correspondence with the results of the present investigation, it was decided instead to use the experimental data to generate the appropriate wake functions.

† Coles normalized ω so that $\omega(1) = 2$.

Wake functions were constructed by subtracting experimental values of w^+ from those calculated using a wall-law expression. Each wake function so obtained was then normalized by a w^+ value from the wall-law expression at $y^+ = \delta^+$. A precise evaluation of δ^+ is somewhat uncertain; however, owing to the flatness of the wall-law curves at large y^+ (e.g. $y^+ \sim 2000$), the value of the normalizing factor is insensitive to uncertainties in δ^+. For this investigation, δ^+ was taken as $2{\cdot}3\delta^+_{\frac{1}{2}}$.

A re-examination of the wall-law data in figure 5 revealed that an expression such as (10) could not adequately account for the effect of the transverse curvature of the surface. Therefore, r_w^+ has to appear as a parameter either in the wall-law expression or in the wake function, or possibly in both.

In an attempt to obtain a wake function which is independent of r_w^+, wall-law expressions were generated by the method proposed by Sparrow *et al.* (1963) wherein there exists a dependence on r_w^+. This procedure is based on momentum exchange coefficients proposed by Deissler & Loeffer (1959), along with the assumption that $\tau \sim 1/r$. Upon subtracting the experimental w^+ values from those of Sparrow *et al.* (1963) the wake functions so generated themselves exhibited a strong dependence on transverse curvature. Other wall-law distributions based on the Prandtl mixing length model proved likewise unsuccessful.

Rather than have both the wall-law expression and the wake function depend on r_w^+, the dependence was confined to the wake function by using the wall-law equation proposed by Coles, that is

$$w^+ = 2{\cdot}5\,(\ln y^+) + 5{\cdot}1. \tag{12}$$

Typical wake functions generated using this expression in conjunction with the experimental data are illustrated in figure 7. Crossplots of these data at three representative values of $y/\delta_{\frac{1}{2}}$, shown in figure 8, indicate a unique dependence of the wake function on r_w^+, independent of the Reynolds number.

Second-degree polynomials of the form

$$\omega = F_1 + F_2(1/r_w^+) + F_3(1/r_w^+)^2, \tag{13}$$

were fitted to the crossplots at several values of $y/\delta_{\frac{1}{2}}$ by the least-squares method. Each of the solid lines in figure 8 actually represents a fit to twenty points rather than to the fewer typical points plotted. The values of F_1, F_2 and F_3 are listed in table 1. By employing (13) in conjunction with table 1, wake functions at arbitrary r_w^+ values can be generated.

The case of $r_w^+ \to \infty$ represents either a plane or a radial wall jet, that is, a flow configuration with no transverse surface curvature. In terms of (13), $\omega = F_1(y/\delta_{\frac{1}{2}})$. In order to assess the universality of this wake function, plane wall-jet velocity profiles were computed for two values of $\delta^+_{\frac{1}{2}}$, 1610 and 2660. These values were selected to correspond to plane wall-jet data reported by Bradshaw & Gee (1960) for stations 6·1 and 22·8 in. downstream of the jet nozzle.† The comparison of

† The use of the Bradshaw & Gee (1960) data as a basis of comparison is supported by the general concensus between the results of that investigation and those of Sigalla (1958).

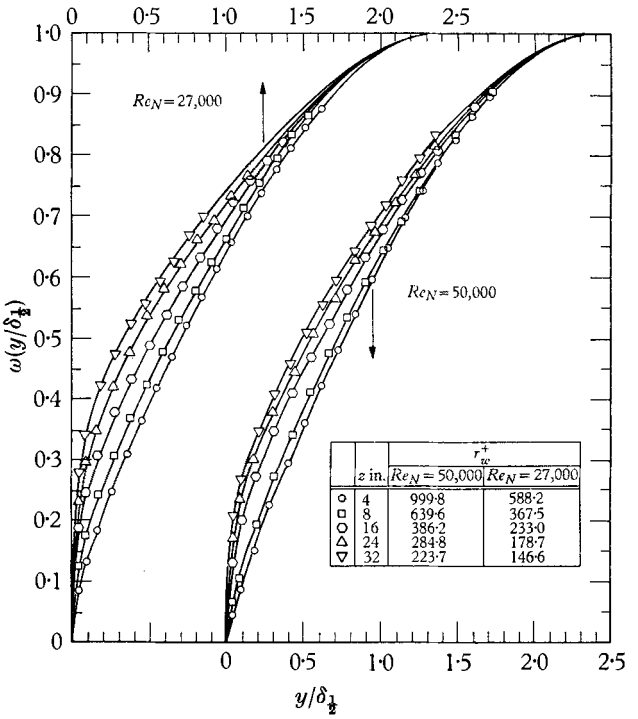

FIGURE 7. Cylindrical wall-jet wake functions.

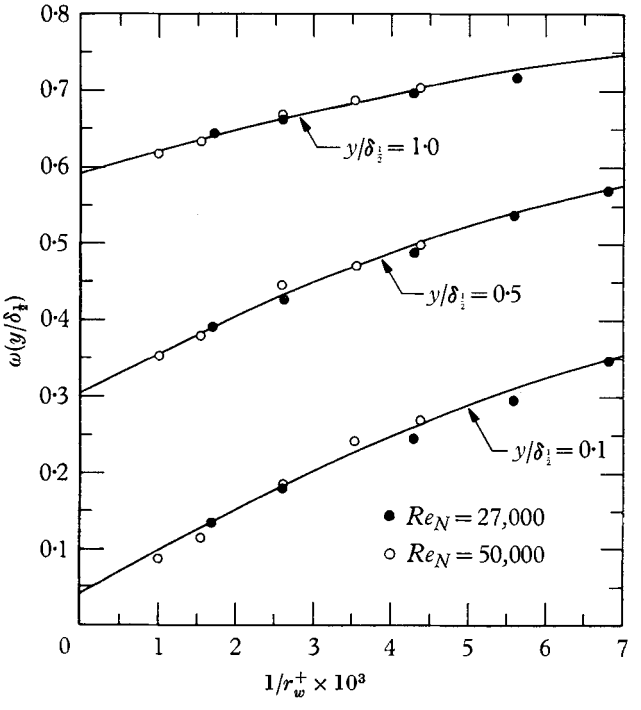

FIGURE 8. Cross-plots of wake function data.

computed and measured velocity distributions pictured in figure 9 shows that the wake function generated herein provides an excellent basis for the prediction of the experimental plane wall-jet data.

In light of the foregoing, it may be concluded that wake functions calculated from (13), utilizing the constants in table 1, provide a means for generating wall-jet velocity profiles where transverse surface curvatures range from an r_w^+ of approximately 125 to ∞ (flat plate).

$y/\delta_{\frac{1}{2}}$	F_1	F_2	F_3
0·05	0·0147	48·0	−1330
0·10	0·0428	59·8	−2312
0·20	0·1105	64·6	−2941
0·30	0·1773	63·3	−2999
0·40	0·2440	57·9	−2580
0·50	0·3048	55·5	−2656
0·60	0·3660	51·4	−2564
0·80	0·4859	39·6	−1743
1·00	0·5934	30·5	−1301
1·20	0·6921	21·7	−827
1·40	0·7786	15·4	−844
1·60	0·8728	−10·7	4753
2·30	1·0000	0	0

TABLE 1. Wake function constants.

The momentum exchange process

Certain characteristics of the momentum exchange process in turbulent wall jets can be ascertained from a knowledge of the transverse distribution of the shear stress. In particular, for a plane turbulent wall jet, Bradshaw & Gee found that the locations of zero shear stress and zero velocity gradient did not coincide, thus

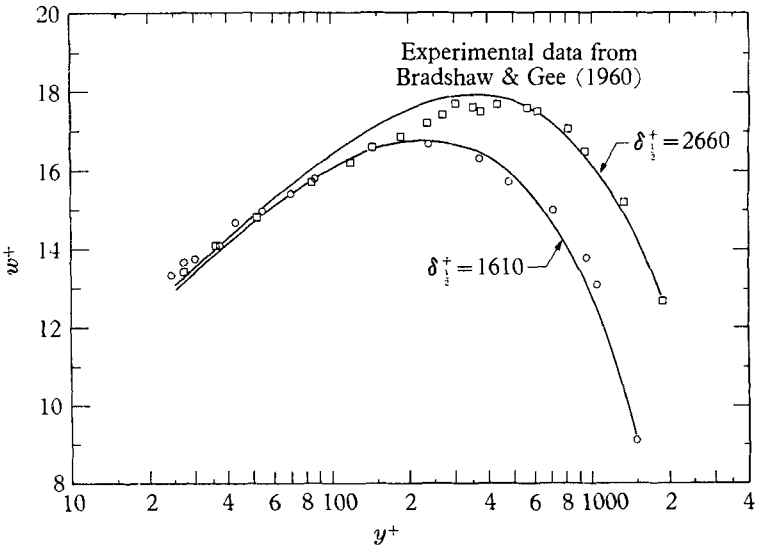

FIGURE 9. Comparison of experimental plane wall-jet data with profiles computed using wake function for $r_w^+ \to \infty$.

negating the utility of the eddy viscosity concept in the neighbourhood of the point of maximum velocity. The potential importance of this finding provided impetus for examining the cylindrical wall-jet data for the existence of a similar phenomenon.

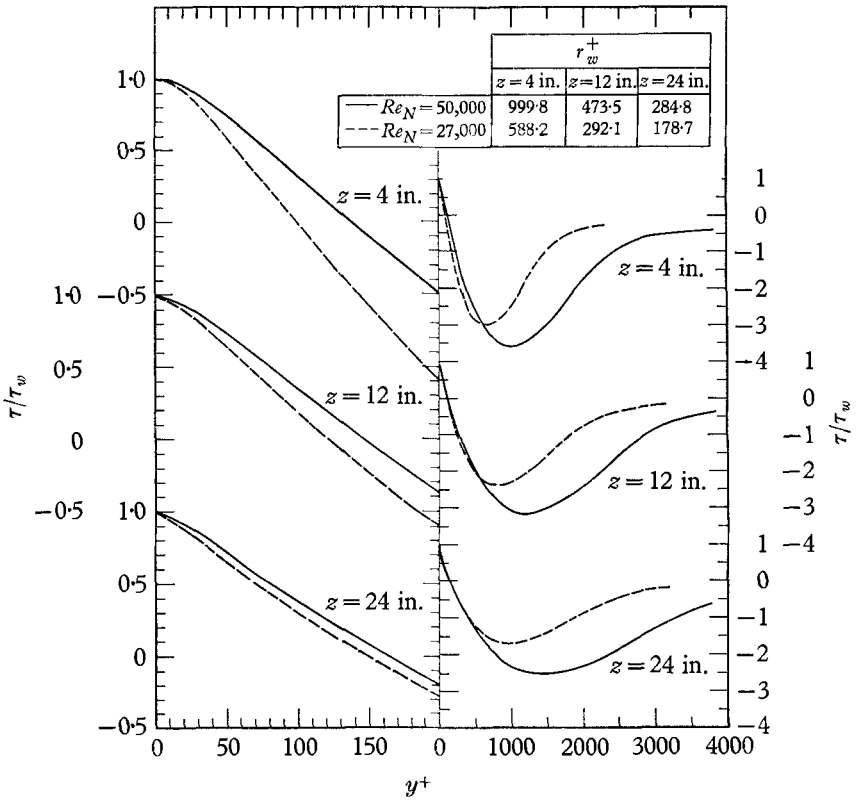

FIGURE 10. Transverse distributions of shear stress.

Transverse distributions of shear stress were generated by incorporating the measured wall shear stress and the velocity profile data in an integral momentum equation. Distributions so obtained are presented in figure 10 and are representative of a total of 20 such curves found in Starr (1966). The curves on the left of figure 10 are for y^+ values that, for the most part, fall within the region $0 \leqslant y \leqslant \delta_m$. Information for large y^+ values is presented on the right of the figure.

In order to explore any possible differences between the locations of zero shear and zero velocity gradient, velocity profile data are plotted in figure 11 for eight axial stations and two nozzle Reynolds numbers. The location of zero shear corresponding to each profile is also indicated. On the basis of these results, it appears that the locations of zero shear and zero velocity gradient are, in some cases, somewhat displaced. However, in all cases, the velocity gradient is relatively small when the shear is zero. Thus, for many purposes, it appears sufficient to assume that the two locations are coincident. Because of the obvious uncertainty

in the locations of maximum velocity owing to the flatness of the profiles, a quantitative estimate of the variance between the two points would have little significance.

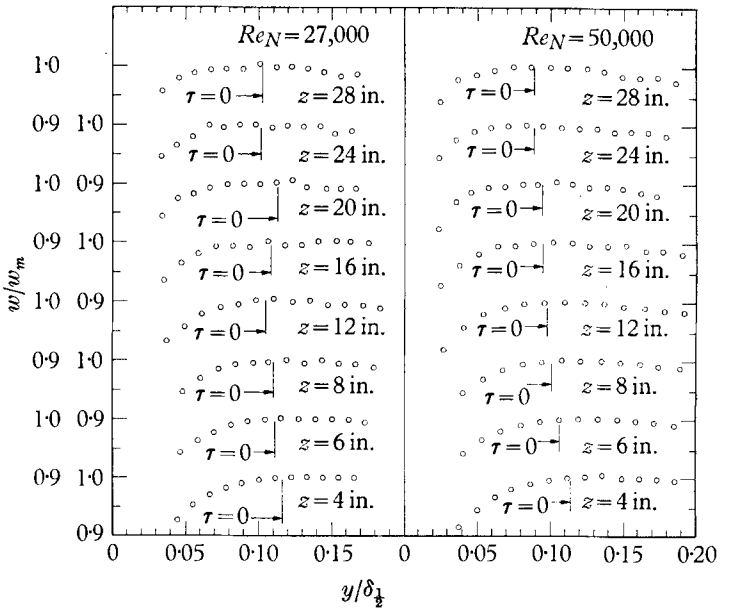

FIGURE 11. Locations of zero shear.

It is of interest to compare the momentum exchange process in the *outer* mixing layer of the cylindrical wall jet with that of a free jet. To facilitate the comparison, eddy viscosities for plane and axisymmetric free jets are first evaluated. Experiments have demonstrated that at sufficient distances from the jet source, free jet widths increase linearly with z and velocity profiles are similar. Thus, for an axisymmetric jet

$$\delta_{\frac{1}{2}} = \sigma z, \quad w/w_m = f(\eta), \quad \eta = r/\delta_{\frac{1}{2}}. \tag{14}$$

With ϵ defined by†

$$\epsilon = \frac{\tau}{\rho \Big/ \left(\dfrac{\partial w}{\partial r}\right)}, \tag{15}$$

and letting

$$f(\eta) = e^{-0{\cdot}692\eta^2}, \tag{16}$$

evaluation of the integral momentum equation for an axisymmetric jet leads to the expression

$$\frac{\epsilon}{w_m \delta_{\frac{1}{2}}} = 0{\cdot}521 \frac{\sigma}{\eta^2}(1 - e^{-0{\cdot}692\eta^2}). \tag{17}$$

By carrying out a similar procedure for a plane free jet, there results

$$\frac{\epsilon}{w_m \delta_{\frac{1}{2}}} = 0{\cdot}386 \frac{\sigma}{\eta} \operatorname{erf}(0{\cdot}832\eta). \tag{18}$$

† The laminar contribution is fully negligible and is omitted.

From experimental data reported by Reichardt (1942), it is found that σ is 0·115 and 0·0848 respectively for the plane jet and for the axisymmetric jet.

The extent to which the momentum exchange process in the outer mixing layer of a cylindrical wall jet resembles that of a free jet can now be explored. To this end, comparisons are made between the eddy viscosities computed from the experimental data and those computed from (17) and (18). It is expected that (17) should apply where $r_w \ll \delta_{\frac{1}{2}}$ and (18) should apply where $r_w \gg \delta_{\frac{1}{2}}$. Hence, the experimental data should fall somewhere between curves generated from the two expressions.

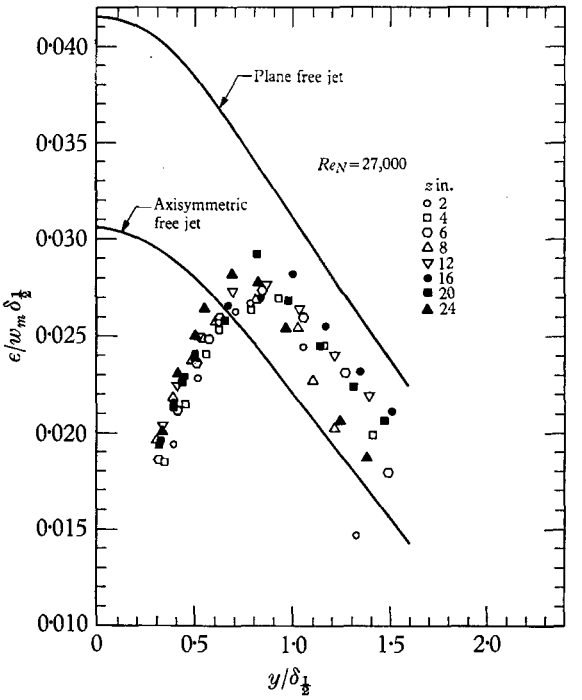

FIGURE 12. Eddy viscosity data.

Experimental eddy viscosity results are shown in figure 12. Similar results are available for $Re_N = 50{,}000$ in Starr (1966). By inspecting the figure, it is seen that the data fall between the two curves when $y/\delta_{\frac{1}{2}} > 0{\cdot}8$. When $y < 0{\cdot}8\delta_{\frac{1}{2}}$, the momentum exchanges process is evidently influenced by the presence of the rod surface, since the eddy viscosity is below that of a free jet.

An interesting finding emerges when one considers that mixing lengths associated with free turbulent jets are approximately $0{\cdot}25\delta_{\frac{1}{2}}$. Hence, if the mixing length near the wall is, as assumed by Prandtl, equal to $0{\cdot}4y$, its value would correspond to that of a free jet when $0{\cdot}4y = 0{\cdot}25\delta_{\frac{1}{2}}$, or when $y = 0{\cdot}625\delta_{\frac{1}{2}}$. This simple computation indicates, as does the experimental eddy viscosity data, that the influence of the wall extends well beyond the point of maximum velocity ($y/\delta_{\frac{1}{2}} \sim 0{\cdot}15$).

REFERENCES

BAKKE, P. 1957 An experimental investigation of a wall jet. *J. Fluid Mech.* **2**, 467.

BRADSHAW, P. & GEE, M. T. 1960 Turbulent wall jets with and without an external stream. *Aero. Res. Counc. Lond. R & M* no. 3252.

BRADSHAW, P. & LOVE, E. M. 1961 The normal impingement of a circular air jet on a flat surface. *Aero Res. Counc. Lond. R & M* no. 3205.

BRIGHTON, J. A. & JONES, J. B. 1964 Fully developed turbulent flow in annuli. *J. Basic Engin.* **86**, 835.

COLES, D. 1956 The law of the wake in the turbulent boundary layer. *J. Fluid Mech.* **1**, 191.

DEISSLER, R. G. & LOEFFER, A. L. 1959 Analysis of turbulent flow and heat transfer on a flat plate at high Mach numbers with variable fluid properties. *NASA Rept.* no. R-17.

FÖRTHMANN, E. 1934 Turbulent jet expansion. *Ing. Arch.* **5**, 42; also *NACA TM* 789.

GLAUERT, M. B. 1956 The wall jet. *J. Fluid Mech.* **1**, 625.

HEAD, M. R. 1958 Entrainment in the turbulent boundary layer. *Aero. Res. Counc. Lond. R & M* 3152.

JONSSON, V. K. 1965 Experimental studies of turbulent flow phenomena in eccentric annuli. Ph.D. Thesis, University of Minnesota.

KLEBANOFF, P. S. & DIEHL, Z. W. 1952 Some features of artificially thickened fully developed boundary layers with zero pressure gradient. *NACA Rept.* no. 1110.

KRUKA, V. & ESKINAZI, S. 1964 The wall jet in a moving stream. *J. Fluid Mech.* **20**, 555.

LAWRENCE, R. L. 1964 Velocity profiles from compressible wall jets. *AIAA J.* **2**, 574.

LUDWIEG, H. 1950 Instrument for measuring the wall shearing stress of turbulent boundary layers. *NACA TM* 1284.

MATHIEU, J. & TAILLAND, A. 1961 Étude d'un jet plan dirigé tangentiellement à une paroi. *C.R. Acad. Sci., Paris*, **252**, 3736.

MATHIEU, J. & TAILLAND, A. 1963 Étude d'un jet plan dirigé tangentiellement à une paroi. *C.R. Acad. Sci., Paris*, **256**, 2768.

MYERS, G. E., SCHAUER, J. J. & EUSTIS, R. H. 1963 Plane turbulent wall jet flow development and friction factor. *J. Basic Engin.* **85**, 47.

REICHARDT, H. 1942 Gesetzmassigkeiten der freien Turbulenz. *VDI-Forschungsheft*, **414**.

SCHWARZ, W. H. & COSART, W. P. 1961 The two-dimensional turbulent wall jet. *J. Fluid Mech.* **10**, 481.

SIGALLA, A. 1958 Measurement of skin friction in a plane turbulent wall jet. *J. R. Aero. Soc.* **62**, 873.

SPALDING, D. B. 1965 A unified theory of friction, heat transfer and mass transfer in the turbulent boundary layer and wall jet. *Aero. Res. Counc. Lond. Current Paper*, no. 829.

SPARROW, E. M., ECKERT, E. R. G. & MINKOWYCZ, W. J. 1963 Heat transfer and skin friction for turbulent boundary layer flow longitudinal to a circular cylinder. *J. Appl. Mech.* **30**, 37.

STARR, J. B. 1966 An experimental investigation of a cylindrical turbulent wall jet. Ph.D. Thesis, University of Minnesota.

TOWNSEND, A. A. 1956 *The Structure of Turbulent Shear Flow.* Cambridge University Press.